J Sol-Gel Sci Technol (2014) 69:155–165
DOI 10.1007/s10971-013-3198-z

ORIGINAL PAPER

Synthesis and characterization of sol–gel derived CNSL based hybrid anti-corrosive coatings

Dinesh Balgude · Kiran Konge · Anagha Sabnis

Received: 1 April 2013 / Accepted: 25 October 2013 / Published online: 31 October 2013

Abstract Thermally cured cashew nut shell liquid based hybrid coatings have been successfully developed using three step processes of malenization, silane modification and subsequent hydrolysis and condensation with tetra ethyl orthosilicate for corrosion protection of mild steel. The synthesized precursor was then characterized by Fourier transform infrared spectroscopy and nuclear magnetic resonance spectroscopy (^{1}H-NMR, ^{13}C-NMR and ^{29}Si-NMR) for structural elucidation. Four different coating formulations were developed on the basis of silane content (5, 10, 15 and 20 %) in the coating and cured with hexabutoxymethylmelamine at 120 °C for 1 h. The completely cured coatings were evaluated for mechanical properties, solvent resistance, chemical resistance, hydrolytic stability and accelerated weathering properties. Scanning electron microscope/energy dispersive spectroscopy was used to analyse the morphological behaviour and elemental distribution of the coating. Results revealed that 20 % silane modification showed better overall properties as compared to other formulations due to formation of more metal–oxygen–silicon covalent bond at metal-coating interface.

Keywords CNSL · Sol–gel · Hybrid coatings · Anti-corrosive · Accelerated weathering tests · SEM/EDX

1 Introduction

Corrosion is a destructive attack of various environments like marine, industrial, urban, rural etc., onto the metal which leads to reduction in the useful properties of metals resulting in direct or indirect losses. Even in developed countries these losses are quite high to the extent of 4–5 % of Gross national product (GNP) of the country. In India, an estimated loss of Rs. 36,000 Crores (US $8 billion) occurs every year due to corrosion and at least 25 % of this could be avoided by using appropriate corrosion-control technology.

One of the generic ways to protect the metal is the ''coating application'' which not only protects them from corrosion but also imparts some aesthetic value. Till date numbers of chemistries have been well reported for anti-corrosive application, some of them being epoxy, alkyds, polyesters, phenolic [1–3] etc. Though these petroleum derived resins have played a vital role in the coating industry, their exponential rising prices and high depletion rate forces the polymer and coating technologist to explore the bio based raw materials for polymer/resin synthesis. The increasing worldwide interest on the use of bio-materials is mainly due to the fact that these materials are derived from natural resources which are abundantly available. Some of the bio based materials include cellulose, starch, sucrose, sugar, lignin, plant and animal oils etc. One such compound is cashew nut shell liquid (CNSL), which is cheap and available in sufficient quantities all over the world for industrial exploitation.

Physically CNSL appears as reddish brown, viscous fluid found in shells of cashew fruits of *Anacardium occidentale*. CNSL is mainly extracted by hot-oil and roasting process in which CNSL oozes out from the shells [4]. The extracted CNSL contains number of useful phenolic derivatives with meta substituted long chain saturated/unsaturated hydrocarbons which make them suitable for number of polymerization reactions through addition as

D. Balgude · K. Konge · A. Sabnis (✉)
Department of Polymer and Surface Engineering, Institute of Chemical Technology, Nathalal Parekh Marg, Matunga (E), Mumbai 400019, India
e-mail: as.sabnis@ictmumbai.edu.in

well as condensation mechanisms. They were used in number of industrial applications like laminating resins, adhesives, ion-exchange resins, paints and coatings, lacquers, hybrid materials, water proofing agent, surface active agents etc. [5–8].

Since almost 10 years, sol–gel derived organic inorganic hybrid coatings are widely used as an effective corrosion protection methodology for metals [9]. They offer an excellent adhesion to metals as well as to the subsequent coat via strong covalent bond and a three dimensional network of –Si–O–Si– linkages which helps to retard the penetration of corrosive medium through the coating [10]. Unlike conventional surface protection methodology, silane based pre-treatment is an environment friendly technology with number of advantages such as room temperature synthesis, chemical inertness, high oxidation and abrasion resistance, excellent thermal stability, very low health hazard etc.

The proposed work deals with the development of novel hybrid precursor from CNSL and their application as an anti-corrosive coating. The combination of bio-based materials and sol–gel technology serves the purpose of environment friendly coatings with improved overall properties.

2 Experimental

2.1 Materials

Cashew nut shell liquid (NC-700) was procured from Cardolite Corporation, Mangalore, 3-glycidyloxypropyl trimethoxysilane (GPTMS) and Tetraethyl orthosilicate (TEOS) were obtained from Wacker Silicones, Mumbai. Maleic Anhydride ($C_4H_2O_3$), anhydrous sodium sulphate (Na_2SO_4), glacial acetic acid (GAA), methanol, methyl ethyl ketone, toluene, *p*-toluene sulfonic acid (*p*-TSA), triethylamine (TEA) were purchased from SD Fine chem. Ltd., Mumbai, hexabutoxymethylmelamine (HBMM) was procured from Shalimar Paints Ltd, Nasik, India.

2.2 Synthesis

CNSL and its derivatives were utilized as such for their chemical modification to synthesize hybrid materials. Chemical modification involved a 3-step process of malenization, silane modification and subsequent hydrolysis and condensation with tetra ethyl orthosilicate for corrosion protection of mild steel. At first, CNSL was analyzed for its physicochemical properties as per ASTM standards as reported in Table 1.

Table 1 Physiochemical characterization of CNSL

Properties	Values	ASTM standards
Appearance	Reddish brown colored liquid	NA
Acid value(mg KOH/g of sample)	8.9–10	D-1980-87 (reapproved 1998)
Iodine value (gram of I_2/100 g of sample)	230	D-5554-95 (reapproved 2011)
% Non-volatile matter	99.96 %	D4140-07 (reapproved 2013)

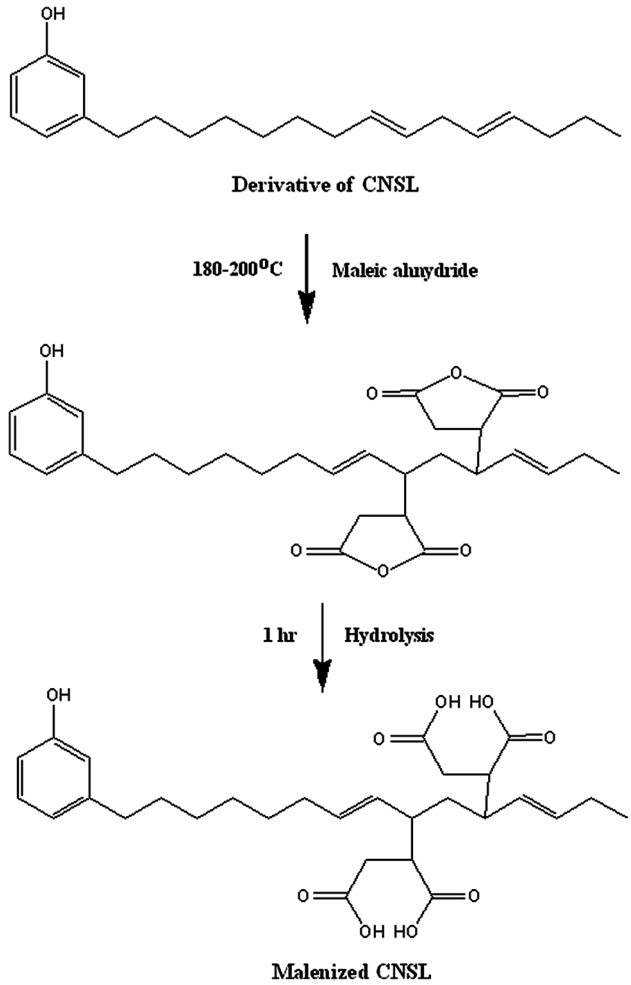

Fig. 1 Malenization of CNSL

2.2.1 *Malenization of cashew nut shell liquid (CSNL)*

The number of unsaturation present in the CNSL was calculated on the basis of Iodine value of CNSL (230 g of I_2/100 g) and it was observed to be 2.74 equivalents. Malenization of CNSL was carried out in the range of 5–20 % on the basis of equivalents of unsaturation present in CNSL. During malenization, the addition reaction takes

Table 2 Reaction conditions of malenization of CNSL

Sr. No.	Batch no.	Amount of CNSL (g)	Amount of maleic anhydride (g)	Temperature (°C)	Time (min)	Acid value (mg KOH/g)
1	MC-5	100	4.44	180–200	240	42.27
2	MC-10	100	8.88	180–200	240	67.56
3	MC-15	100	13.32	190–210	220	90
4	MC-20	100	17.76	190–210	200	130

place between maleic anhydride ($C_4H_2O_3$) and unsaturation present in methylene linkage of CNSL. A substituted succinic anhydride is formed by transfer of a hydrogen atom [11] from unsaturated methylene linkage to the maleic anhydride as shown in Fig. 1. After maleinization of CNSL, hydration was carried out by boiling maleinized CNSL in water for 1 h. Hydration results in the opening of the anhydride rings. The excess water was distilled off under reduced pressure followed by passing the product over anhydrous Na_2SO_4 to remove the water traces. The malenized CNSL was then characterized for its Acid value (as reported in Table 2). The detailed compositions of malenization reaction using various percentages of maleic anhydride are described in Table 2 along with reaction time and reaction temperature. The reaction time for all the batches was optimized considering no gelation during malenization reaction, as chances of gelation increase on increasing the content of maleic anhydride[12].

2.2.2 *Synthesis of malenized CNSL based hybrid precursor (MCHP)*

Silane modified malenized CNSL was then synthesized by reacting 20 % malenized CNSL (MC-20) with GPTMS at 60–70 °C for 4 h under magnetic stirring. The reaction was catalyzed by addition of triethylamine (0.2 wt%). GPTMS was added from 5 to 20 wt% on basis of carboxyl content (Acid value) of MC-20. The purpose of selecting MC-20 to synthesize the hybrid precursor was to have the maximum advantage of functionality during curing reaction. With higher acid value, the carboxyl functionality would be more and subsequently more will be the crosslinking during curing reaction. The synthesized hybrid precursors were coded as MCHP-5 %, MCHP-10 %, MCHP-15 %, and MCHP-20 % where MCHP stands for malenized CNSL based hybrid precursor and the number denoted as the percentage of GPTMS modification. Chemical structure of malenized CNSL based hybrid precursor (MCHP) is shown in Fig. 2.

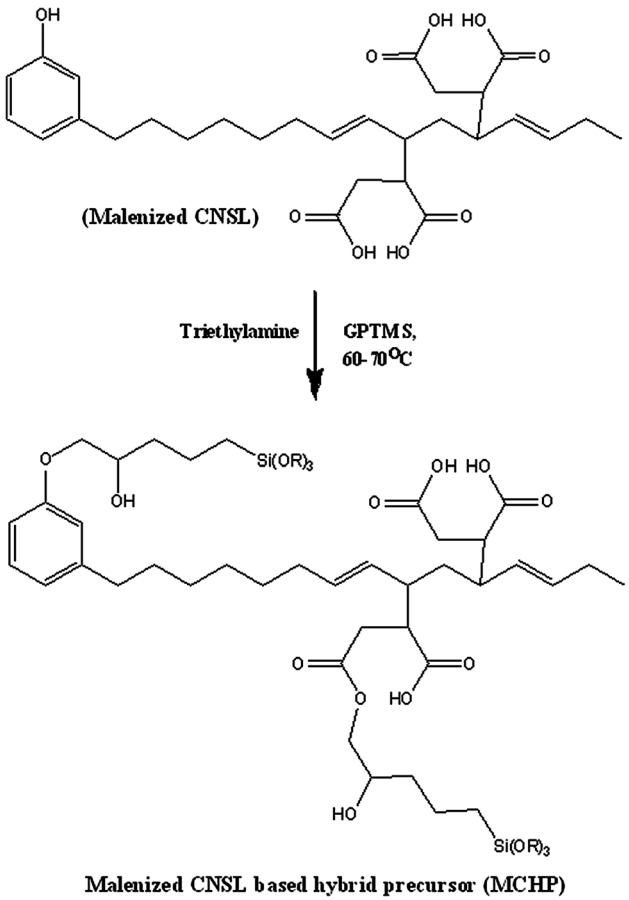

Fig. 2 Malenized CNSL based hybrid precursor (MCHP)

2.3 Coating preparation

The primary sol was then synthesized by hydrolyzing the mixture of TEOS and MCHP along with methanol at room temperature (30 °C) under magnetic stirring at a rate of 150 rpm for 24 h. TEOS and methanol (MeOH) were added with respect to GPTMS content in MCHP (molar ratio of TEOS/GPTMS/MeOH = 1/2/2). An electronic pH meter(Digital pH Meter Model: pH 600, Sigma Instruments) was used to monitor the pH of solution which was maintained in the range of 2–4 using diluted solution of Glacial acetic acid (GAA) (0.05 M) [13]. GAA was added with respect to total reaction solids (1 wt% of reaction solids). For all the formulations, hydrolysis rate (molar ratio of $H_2O/Si = 15:1$) and % non-volatile matter (%NVM = 75) was maintained constant. Ethanol was used as a solvent to maintain the % NVM. The coating solutions were formulated by mixing primary sol and HBMM as a crosslinker in a ratio of 70:30 wt%, respectively. The

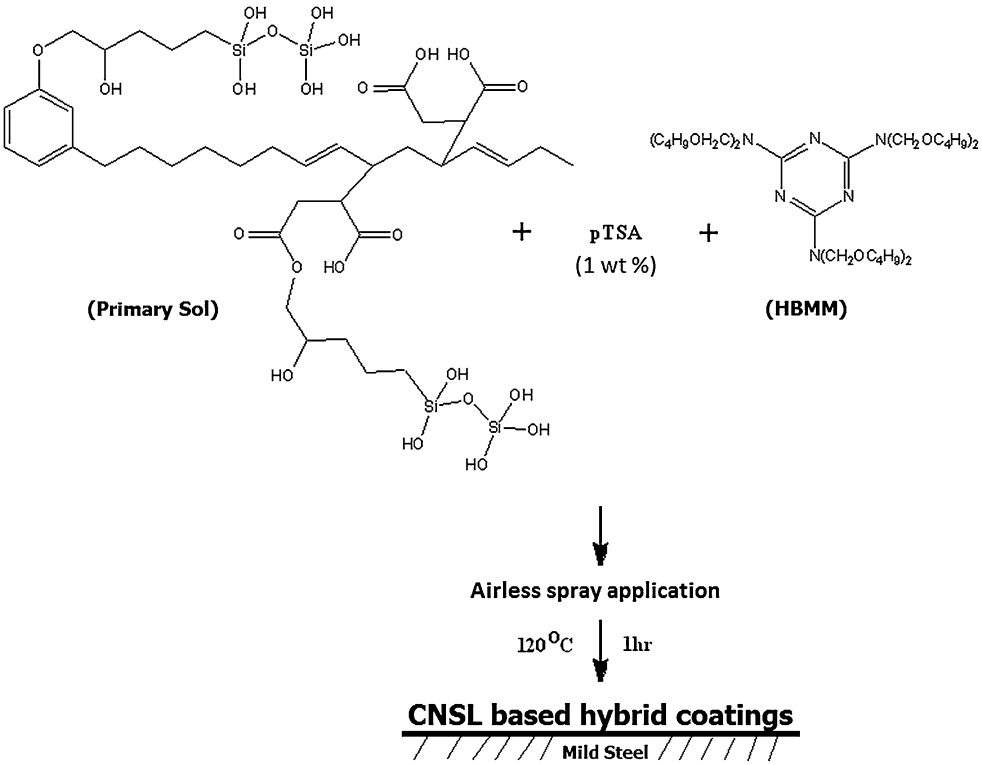

Fig. 3 Schematic representation of CNSL based hybrid coatings

reaction between primary sol and HBMM was catalyzed by addition of 1 wt% of *p*-TSA. The reaction scheme for CSNL based hybrid coatings is shown in Fig. 3.

2.4 Surface preparation, coating deposition and curing of hydrolyzed MCHP with HBMM resin

Mild steel panels were manually cleaned before application. Cleaning involved degreasing, hand scrubbing using emery paper (120 no.) followed by methanol cleaning. The application viscosity of all the coating solutions was maintained at 40 % NVM using mixture of xylene and butanol in 70:30 wt% ratios. The coating solutions were deposited onto prepared substrate by conventional airless spray application according to ASTM D 4708-99. The coated substrates were allowed to air dry for 10 min and were then placed in an air circulating oven to cure at 120 °C for 1 h. The typical dry-film thickness of coating was observed to be in the range of 50–60 microns. Completely cured panels were evaluated for mechanical, solvent and chemical resistance properties, hydrolytic stability, accelerated weathering and electrochemical properties as per ASTM standards.

3 Methods and measurements

The malenization of CNSL and subsequent hydrolysis was characterized for presence of functional groups by Fourier Transform Infrared Spectroscopy (FTIR) in the spectra range of 400–4,000 cm^{-1} on Perkin-Elmer Spectrum 100 Instrument as per ASTM E-1252. Further, the prepared primary sol was characterized by nuclear magnetic resonance spectroscopy (^{1}H-NMR, ^{13}C-NMR and ^{29}Si-NMR) for structural elucidation on Mercury Plus NMR spectrometer at 400 MHz using deuterated chloroform as solvent and tetramethylsilane (TMS) as an internal standard.

Applied coatings were evaluated for adhesion properties by cross cut adhesion with commercial cellophane tape (25-mm wide semitransparent tape manufactured by Permacel, New Brunswick, NJ 08903) according to ASTM D-3359. Pencil hardness of the coating was measured on hardness tester according to ASTM D-3363. Flexibility and load distribution property of the coating were tested by conical mandrel and impact tester as per ASTM D-522 and ASTM D-2794 respectively. Impact resistance was measured on the impact tester with maximum height of 60 cm and load of 1.36 kg. The solvent resistance of the coatings was evaluated by immersing the coated panel in methanol, methyl ethyl ketone and toluene separately for 4 h. Similarly, the chemical resistance properties of the coatings were evaluated by dipping the coated panels in 5 % HCl and 5 % NaOH for 4 h, respectively. After testing, coated panels were evaluated for degree of adhesion and visual inspection for blisters and cracks, if any. Completely cured coatings were tested for their hydrolytic stability as per ASTM-B-1308. The coated panel was immersed in boiling water for 4 h and was evaluated for loss of adhesion and blister formation, if any.

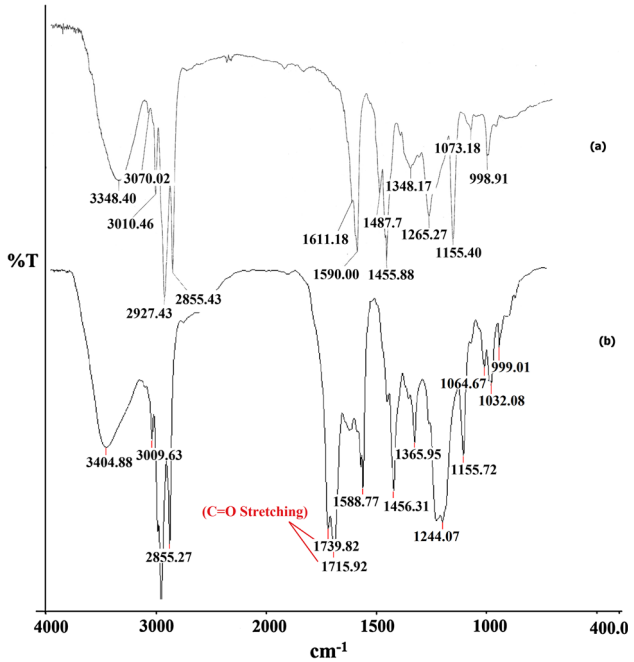

Fig. 4 FTIR spectra of (*a*) CNSL and (*b*) malenized CNSL (after hydrolysis)

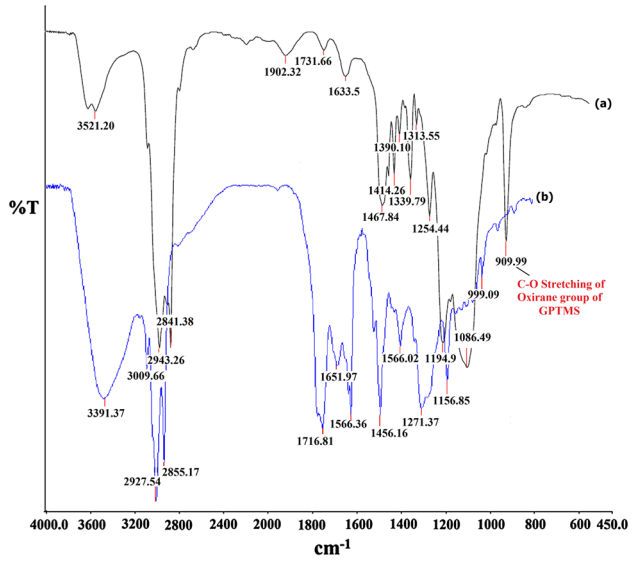

Fig. 5 FTIR spectra of (*a*) GPTMS and (*b*) GPTMS modified malenized CNSL (MCHP)

Accelerated weathering tests like salt spray resistance (ASTM B-117) and UV resistance (ASTM-G53) were carried out to evaluate the anticorrosive performance and outdoor weatherability of the coated panels respectively. The electrochemical properties of the coatings were also evaluated using Tafel polarization studies and electrochemical impedance spectroscopy (EIS) on VersaSTAT-3 instrument (AMETEK, Princeton Applied Research, Oak Ridge, TN). Three-electrode system was used, in which saturated calomel electrode, a platinum electrode and a coated panel acts as reference, counter and working electrode respectively. Electrode surface area exposed to testing solution (3.5 wt% NaCl) was 7 cm^2 in all the cases. All the electrochemical measurements were carried out at room temperature (32 °C) in 3.5 % NaCl solution.

Surface morphology and elemental distribution across the coating was characterized by scanning electron microscope (SEM) and Energy Dispersive Spectroscopy (EDAX) using Quanta 200 SEM instrument (FEI Company, USA).

4 Results and discussion

4.1 Spectroscopic analysis

4.1.1 FTIR analysis

The malenization of CNSL and subsequent hydrolysis was confirmed by FTIR and compared with CNSL spectrum. Figure 4 Shows the appearance of transmission band at 1,715 and 1,740 cm^{-1} corresponding to C=O stretching from carboxylic (–COOH) group after anhydride ring opening due to hydrolysis which was absent in CNSL spectrum. Figure 5 shows the FTIR spectra of GPTMS modified hydrolyzed malenized CNSL and neat GPTMS. The disappearance of peak at 909 cm^{-1} due to C–O stretching of oxirane group of GPTMS confirmed the complete utilization of oxirane group by acidic group of malenized CNSL.

Figure 6 shows the FTIR spectra of CNSL based hybrid coating containing various percentages of MCHP. The graph shows increase in intensity of peaks at 550, 1,017, 1,084, and 1,261 cm^{-1} which corresponds –Si–O–Fe– [14], –Si–O–Si– [15], –Si–O–CH_3 and Si–C [16] respectively on increasing the GPTMS concentration. The increased intensity of Si–O stretching in above mentioned linkages indicates that the condensation reactions have occurred between silanol and metal substrate leads to formation of strong covalent bond at metal coating interface. The increased silicon–oxygen–metal (–Si–O–Fe–) linkages improved the adhesive forces at the metal coating interface, while increased siloxane linkages (–Si–O–Si–) provided enhanced barrier layer for the ingress of aggressive chemicals and hence improved corrosion protection.

Frequency at 3,661 cm^{-1} denoted the existence of OH groups. The sharp peaks at 2,924 cm^{-1} and around 2,884 cm^{-1} are due to –CH_3 symmetric stretching and O–CH_3 asymmetric stretching vibrations. The absorption band at 1,740 cm^{-1} corresponds to –C=O stretching of carboxyl group. The weak peak at 1,558 cm^{-1} and a broad peak at 1,261 cm^{-1} are attributed to –C–N stretching of HBMM and Si–C symmetric bending of Si–CH_3 group respectively.

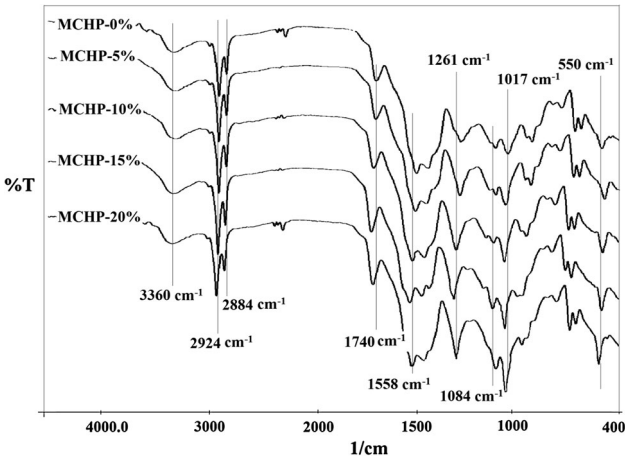

Fig. 6 FTIR spectra of CNSL based hybrid coatings containing various percentages of MCHP

4.1.2 NMR analysis

Further the prepared primary sol was characterized by NMR spectroscopy. The representative ^{1}H-NMR spectrum of prepared primary sol (Fig. 7) shows chemical shift (ppm) of 1.3–1.6 (–CH_2); 5.48 (–CH–); 7.1–7.3 (–C_6H_6). The signals at chemical shifts 11, 3.58 and 5 ppm represent proton from carboxylic, alcoholic and silanol groups respectively, confirmed the malenization of CNSL followed by GPTMS modification. Also, ^{13}C-NMR spectrum of prepared primary sol (Fig. 8) shows peaks for carbon from –CH_2, –CH– of aliphatic unsaturation and from aromatic ring at 29.3–36, 132.4–133.1, 111.6–129.1 and 142.3–157.2 ppm, respectively. This represents structure of CNSL having unsaturated aliphatic chain. The chemical shift (ppm) at 172.0–177.3, 42.3–42.6 and 70.5–71.2 represents carbon from –COO, –CH– from maleic anhydride and –CH– attached to free hydroxyl. This confirmed the malenization and subsequent GPTMS modification of CNSL.

The peak assignments in ^{29}Si-NMR spectra of primary sols are described as previously reported by Derouet et al. for various alkenyl-bonded silica gels [17]. The spectra (as shown in Fig. 9) shows distinct peaks for the silica network units at −49.2 to −50.5 ppm [T^1], −55.9 to −59.6 ppm [T^2], and 65.3 to −68.9 ppm [T^3] which corresponds to R–$Si(OR)_2(–O)_1$, R–$Si(OR)(–O)_2$, R–$Si(–O)_3$ respectively. Also, the spectra shows some low intensity peaks at −93.5 to −94.3 ppm [Q^2], −102.5 to −103.7 ppm [Q^3], and −111.4 to −113.5 ppm [Q^4] attributed to $Si(OSi)_2(OH)_2$, $Si(O-Si)_3(OH)$, and $Si(OSi)_4$, respectively. This could be due to formation of mono, di, tri or tetra siloxane linkages in the matrix. Thus, ^{29}Si-NMR measurements confirmed the formation of a dense siloxane network evident from increasing peak ratios of T^2/T^3 and Q^2/Q^3 on increasing the content of GPTMS (Fig. 9). This indicated the enhancement in the degree of condensation in the sol. The increased degree of condensation has led to the formation of higher reticulated network of TEOS and GPTMS into the hybrid silane matrix.

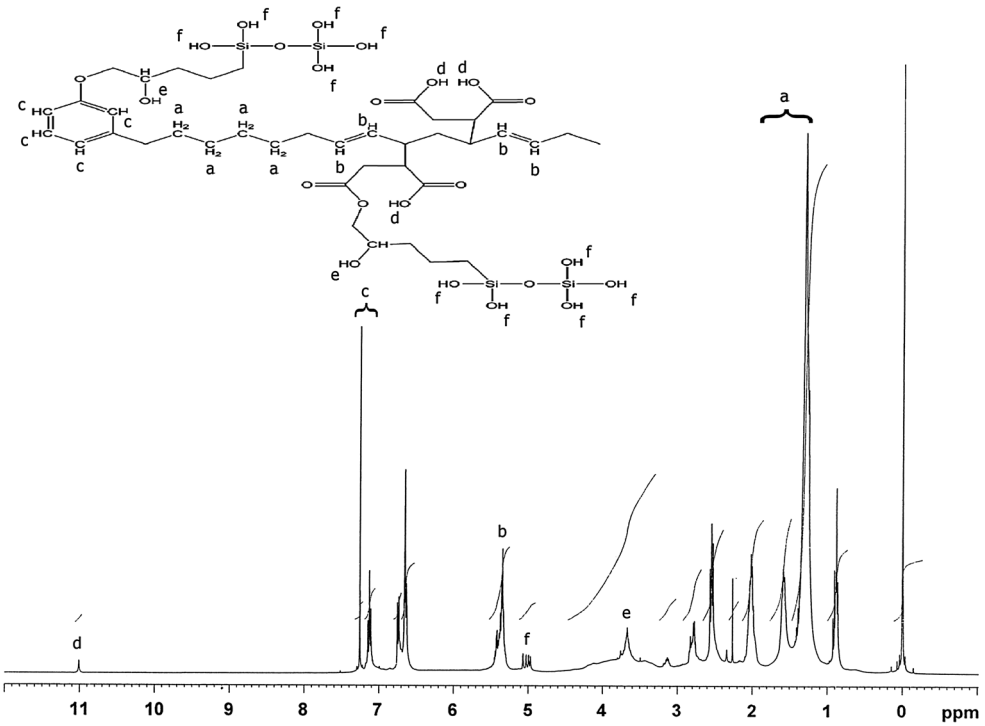

Fig. 7 ^{1}H-NMR spectra of primary sol

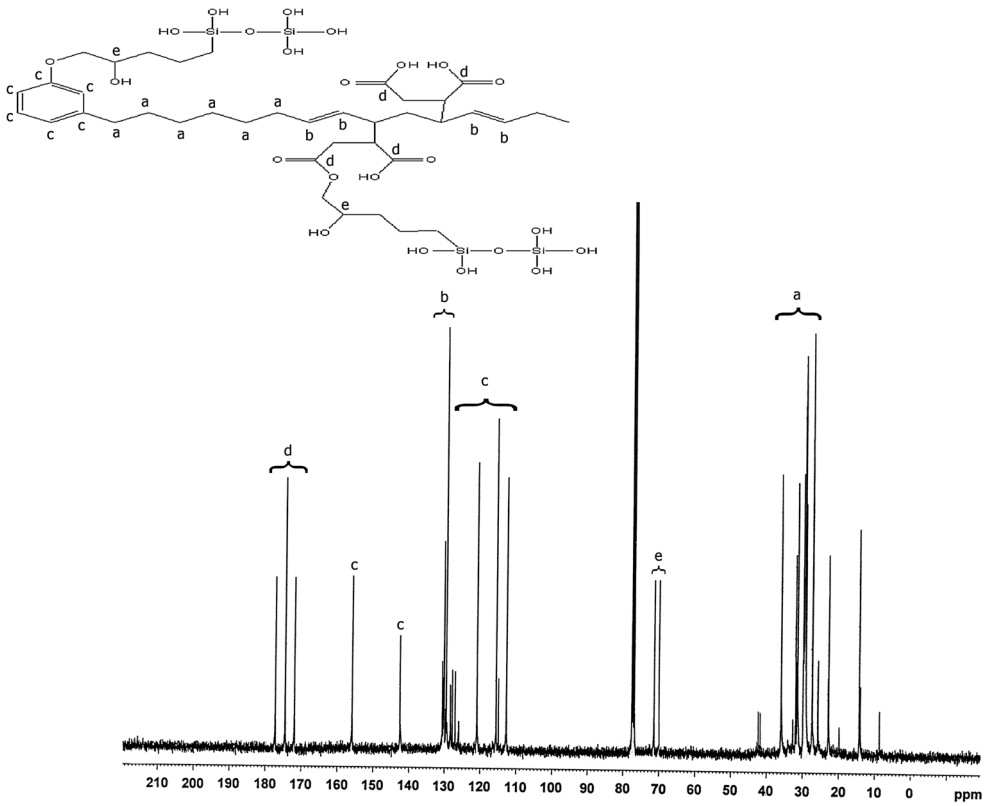

Fig. 8 ^{13}C-NMR spectra of primary sol

4.2 Chemical analysis

Hydrolyzed malenized CNSL was characterized for their Acid value as reported in Table 2. Acid value is a measure of carboxyl content present in the given molecular structure as per ASTM D-1980. On increasing the percentage of malenization, the content of maleic anhydride in a malenized CNSL increases which further increases the carboxyl content of the malenized CNSL. This was reflected in the Table 2 which shows increasing trend for Acid value of malenized CNSL on increasing the percentage of maleic anhydride with highest value of 130 mg of KOH/g for MC-20 (20 % malenization).

Further the GPTMS modification of MC-20 was characterized by measuring the Acid value of reaction mixture before the start of reaction and after completion of reaction. The Acid value of reaction mixture containing MC-20 and GPTMS was observed to be decreased from initial 117 to 93 mg of KOH/g at the end of GPTMS modification reaction. This confirmed the consumption of carboxyl group to open the oxirane group of GPTMS.

4.3 Mechanical properties

The cross hatch adhesion as well as flexibility was observed to be excellent in all the coatings irrespective of the percentage of GPTMS modification. This could be due

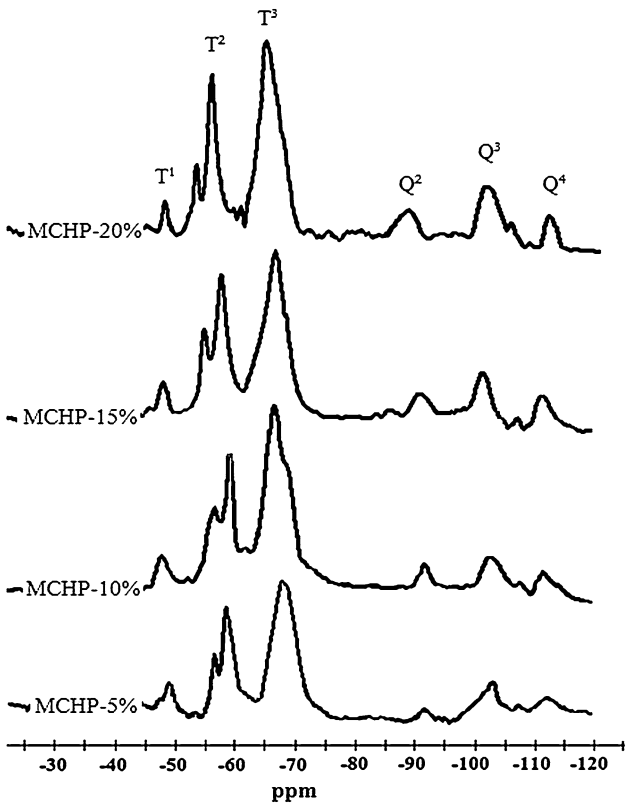

Fig. 9 ^{29}Si-NMR Spectra of primary sols

Table 3 Mechanical properties of CNSL based hybrid coating

Formulation (%)	Dry film thickness (μm)	Adhesion (B)	Flexibility (mm)	Impact (in.-lb)	Pencil hardness
MCHP-0	49–54	5	0	70.86	B
MCHP-5	50–56	5	0	70.86	F
MCHP-10	47–53	5	0	70.86	H
MCHP-15	49–54	5	0	70.86	2H
MCHP-20	48–55	5	0	70.86	2H

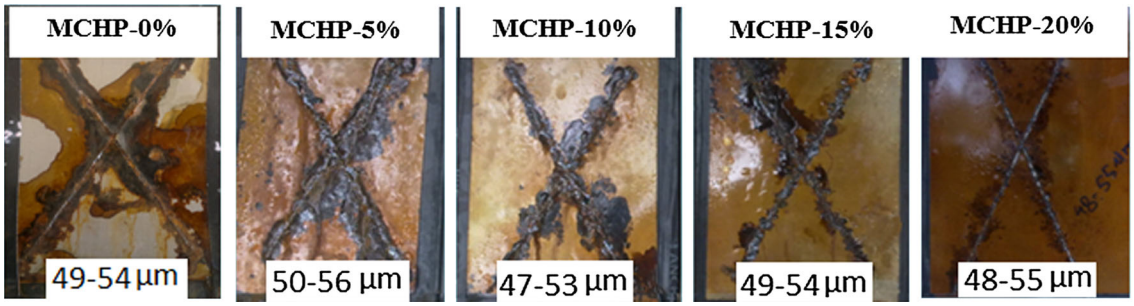

Fig. 10 Salts spray images of CNSL based hybrid coatings after 200 h of exposure in 3.5 % NaCl solution

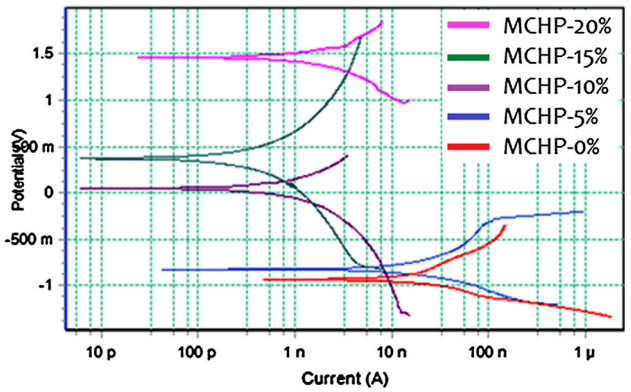

Fig. 11 Potentiodynamic polarization curves of CNSL based hybrid coatings in 3.5 % NaCl

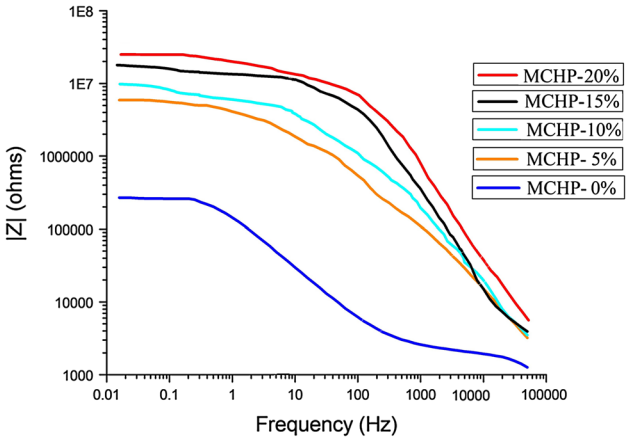

Fig. 12 Bode plots of CNSL based hybrid coatings in 3.5 % NaCl

Table 4 Potentiodynamic polarization data of CNSL based hybrid coatings in 3.5 wt% NaCl solution

Formulation (%)	I_{corr} (μA)	E_{corr} (mV)	Corrosion rate (mmpy)
MCHP-0	2.18×10^{-2}	−0.824	5.56×10^{-5}
MCHP-5	4.29×10^{-11}	−0.934	3.01×10^{-5}
MCHP-10	8.13×10^{-12}	0.046	1.45×10^{-6}
MCHP-15	6.14×10^{-12}	0.367	2.39×10^{-7}
MCHP-20	1.84×10^{-14}	1.562	5.48×10^{-8}

to the presence of long methylene linkages present in CNSL which would take care of any increased crystallinity with increasing GPTMS modification. However; the pencil hardness was observed to be increased with increasing percentage of GPTMS. This may be due to increasing percentage of GPTMS resulting in dense cross-linked polymer network. The impact resistance measured by falling ball impact method was observed to be excellent with impact resistance of 70.86 in.-lb for both intrusion and extrusion modes for all the formulations. Table 3 shows the obtained results of the mechanical properties for all coating samples evaluated.

4.4 Solvent and chemical resistance

The film integrity of the coated panels was evaluated in methanol, methyl ethyl ketone and toluene respectively by

immersion method for 4 h. Similarly, acid and alkali resistance test was carried out according to ASTM D-1308. After 4 h of immersion, all coated panel shows no blister or pit formation in solvent and acid resistance. However, slight blistering was observed in case of alkali dip.

4.5 Hydrolytic stability

After completion of 4 h immersion in boiling water, the panels were dried and observed for film defects. The unaffected secondary adhesion and no film defects for coating formulation MCHP-15 % and MCHP-20 % confirmed their superior hydrolytic stability compared to MCHP-5 % and MCHP-10 %. This could be due to increased silane content resulting in increased Si–O–C linkages which are hydrolytically more stable. The strong siloxane linkages (–Si–O–Si–) formed after condensation between TEOS and GPTMS would also contribute for excellent hydrolytic stability. The coating formulations MCHP-5 % and MCHP-10 % showed inferior hydrolytic stability with weaker secondary adhesion.

4.6 Corrosion resistance of coatings

The corrosion resistance properties of all the coated panels were evaluated as per ASTM B-117 for salts spray resistance. The results after 200 h of exposure revealed that MCHP-20 % showed better corrosion resistance properties compared to other formulations as shown in Fig. 10. This may be due to increased silane content of the coatings with increased siloxane linkages (–Si–O–Si–) which are quite stable to electrolytic environment. However, in MCHP-20 %, slight corrosion of metal surface was observed near the cross area due to its exposure to corroding environment.

The potentiodynamic polarization studies and electrochemical impedance spectroscopy (EIS) were used to evaluate the anticorrosive performance of the coatings. From the polarization curves in the 3.5 % NaCl solution, it can be seen that the corrosion current for the MCHP-0 % formulation is quite larger than that of the other formulations. The incorporation of GPTMS resulted in lower current densities which showed continuous decreasing trend with further increasing GPTMS content. The decreased Icorr (μA) values and corrosion rate (mm/year) with increasing GPTMS content indicated that more siloxane linkages indeed could provide a physical barrier for blocking the electrochemical process. Also, Fig. 11 shows the highest electrochemical potential (ECP) value for MCHP-20 % formulation. This could be due to the presence of pendant hydroxyl group after hydrolysis which participates in electrochemical reactions through the lone pair of electrons available with oxygen atom in hydroxyl group. Table 4 shows the electrochemical parameters, derived from potentiodynamic polarization studies of the coated steel panels.

Figure 12 shows a typical Bode plot for all the formulations. Generally, higher Z modulus at lower frequency indicates a better corrosion resistant coating on the metal substrate [18]. The Bode plot shows higher Z modulus values for MCHP-20 % formulation. This further suggests that the level of porosity and defects present in the developed coatings is very low, which helps to explain the corrosion protection enhancement.

4.7 UV resistance of the coatings

The UV resistance of the coated specimen were evaluated using alternate cycles of UV light and condensation as shown in Fig. 13. Damage caused by the weathering cycle was assessed using visual assessment and gloss measurement. The coated specimens were exposed for 350 h. Visual examination of the exposed specimen shows that 20 % GPTMS modification performed better as compared to other specimens in terms of corrosion products on the surface and cracking or loss of adhesion. Gloss retention of the 20 % formulation was observed to be 79.56 %.

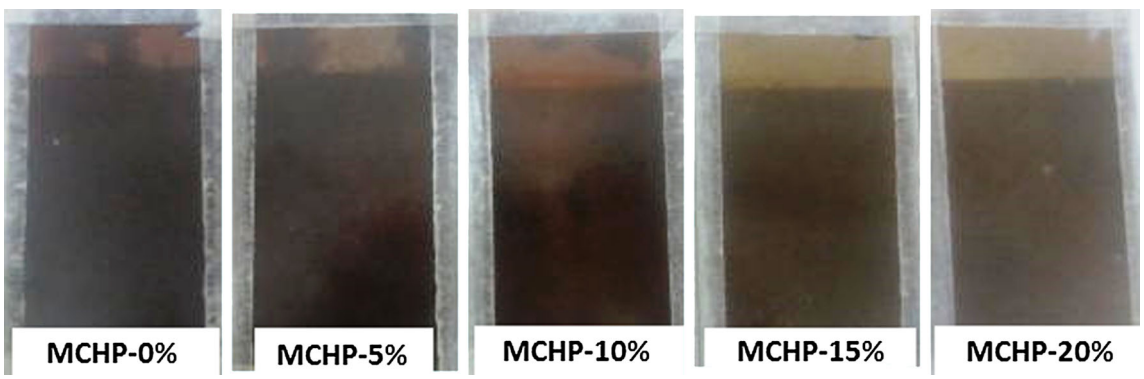

Fig. 13 UV resistance of CNSL based hybrid coatings after 350 h of exposure to 4 h alternate cycles of UV light and condensation

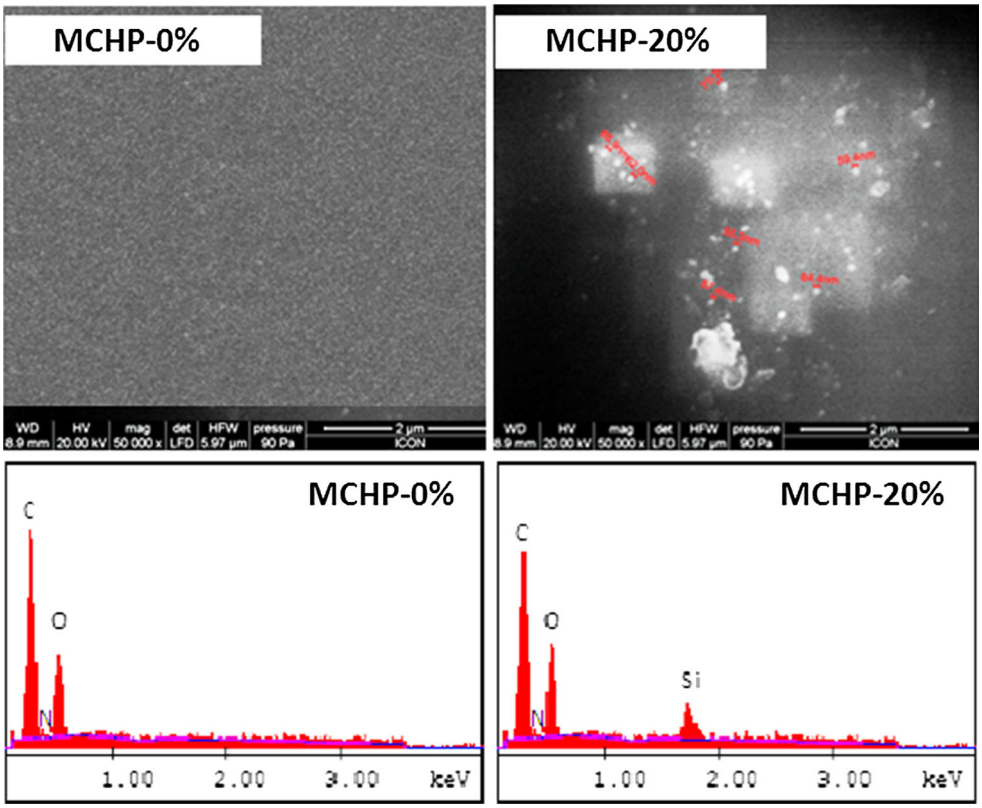

Fig. 14 SEM micrograph of MCHP-0 % and MCHP-20 % coatings

4.8 Scanning electron microscopy (SEM) and energy dispersive spectroscopy (EDAX)

The surface morphology of MCHP-0 % and MCHP-20 % coatings was evaluated by scanning electron microscope using Quanta 200 SEM instrument (FEI Company, USA). The SEM micrographs revealed that the coating on mild steel is uniform, homogenous, and crack free. The EDAX graphs shows uniformly distributed silica with peak at 1.79 keV in MCHP-20 % unlike in MCHP-0 % (as shown in Fig. 14). This confirmed the presence of silica in MCHP-20 %.

5 Conclusion

CNSL based hybrid coatings were developed and their performance in terms of corrosion resistance, UV-resistance, mechanical properties, chemical resistance, solvent resistance and hydrolytic stability were evaluated. All mechanical, chemical and solvent resistance properties were found to be similar for all the coatings except the increasing trend in pencil hardness with increasing GPTMS content which could be due to increased cross-linking density. Silicone modification increased the corrosion and UV-resistance of the system. Significant decrease in corrosion current (1.84×10^{-14} μA) and corrosion rate (5.48×10^{-8} mmpy) was observed for 20 % GPTMS modified malenized CNSL coating compared to other formulations. Improvement in corrosion resistance is attributed to the formation of more number of siloxane linkages (Si–O–Si) at metal coating interface which was also confirmed with ^{29}Si-NMR which helps to improve the barrier property of the system. Also, IR spectra showed an increased intensity of siloxane (–Si–O–Si–) linkages and –Si–O–Fe– linkages on increasing GPTMS concentration. Furthermore, the combination of long chain methylene linkages of CNSL and the presence of siloxane (Si–O–Si) moieties after GPTMS modification of malenized CNSL in the coatings maintained the good balance between flexibility and hardness of the coating. Thus, CNSL can be one of the potential alternatives to few of the petroleum based raw materials, to be used in anti-corrosive hybrid systems with increased corrosion resistance properties without affecting the other properties.

Acknowledgments The authors sincerely acknowledge Cardolite Corporation, Mangalore and Shalimar Paints Ltd, Nashik for their kind support for raw materials supply and testing facilities respectively. Authors also would like to express their sincere gratitude to Dr. Swapan K. Ghosh (Director-NSCC, India) for their kind support in carrying out various analyses with fruitful discussion.

References

1. Monetta T, Bellucei F, Nicodemo L, Nicolais L (1993) Prog Org Coat 21:353–369
2. Bieganska B, Zubielewicz M, Smieszek E (1987) Prog Org Coat 15:33–56
3. Araujo WS, Margarit ICP, Mattos OR, Fragata FL, Lima-Neto PD (2010) Electrochim Acta 55:6204–6211
4. Caplan S (1949) US Patent 2 480 221
5. Balgude D, Sabnis A (2013) J Coat Technol Res. doi:10.1007/s11998-013-9521-3
6. Bhunia HP, Nando GB, Basak A, Lenka S, Nayak PL (1999) Eur Polym J 35:1713
7. Patel RN, Bandyopadhyay S, Ganesh A (2006) J Chromatogr A 1124:130
8. Gedam PH, Sampathkumaran PS (1986) Prog Org Coat 14:115–157
9. Wang D, Bierwagen GP (2009) Prog Org Coat 64:327–338
10. Balgude D, Sabnis A (2012) J Sol–Gel Sci Technol 64:124–134
11. Payne FH (1954) Organic coating technology, vol 1. Wiley, New York, p 48
12. Nakayama Y (1973) US Patent 3 778 418
13. Khramov AN, Balbyshev VN, Voevodin NN, Donley MS (2003) Prog Org Coat 47:207
14. Rossman GR (1988) Rev Mineral 18:193
15. Li C, Wilkes CL (2001) Chem Mater 13:3663
16. Gupta G, Pathak SS, Khanna AS (2012) Prog Org Coat 74:106–114
17. Derouet D, Forgeard S, Brosse JC, Emery J, Buzare JY (1998) J Polym Sci A: Polym Chem 36:437–453
18. Kathalewar M, Sabnis A, Waghoo G (2013) Prog Org Coat 76:1215–1229